Structural study of the T(#)2-LixCoO2 (0.52 < x <= 0.72) phase

ARTICLE *in* INORGANIC CHEMISTRY · FEBRUARY 2004

Impact Factor: 4.76 · DOI: 10.1021/ic026285t · Source: PubMed

6 AUTHORS, INCLUDING:

Dany Carlier
Institut de Chimie de la matière condensée d…
98 PUBLICATIONS **1,508** CITATIONS
SEE PROFILE

Laurence Croguennec
Institut de Chimie de la matière condensée d…
128 PUBLICATIONS **3,309** CITATIONS
SEE PROFILE

Gerbrand Ceder
University of California, Berkeley
503 PUBLICATIONS **21,037** CITATIONS
SEE PROFILE

Inorg. Chem. **2004**, *43*, 914–922

Structural Study of the T#2-Li_xCoO_2 ($0.52 < x \leq 0.72$) Phase

D. Carlier,[†,‡] L. Croguennec,*[,†] G. Ceder,[‡] M. Ménétrier,[†] Y. Shao-Horn,[†] and C. Delmas[†]

Institut de Chimie de la Matière Condensée de Bordeaux—CNRS and Ecole Nationale Supérieure de Chimie et Physique de Bordeaux, Université Bordeaux I, 87 av. Dr. A. Schweitzer, 33608 Pessac cedex, France, and Department of Materials Science and Engineering, Massachusetts Institute of Technology, 77 Massachusetts Avenue, Cambridge, Massachusetts 02139

Received December 19, 2002

The metastable O2-$LiCoO_2$ phase undergoes several reversible phase transitions upon lithium deintercalation. The first transition leads to an unusual oxygen stacking in such layered compounds. This stacking is found to be stable for $0.52 < x \leq 0.72$ in Li_xCoO_2 and is called T#2. We studied this phase from a structural viewpoint using X-ray and neutron diffraction (ab initio method). The new stacking derives from the O2 one by gliding every second CoO_2 slab by ($^1/_3$, $^1/_6$, 0). The lithium ions are found to occupy very distorted tetrahedral sites in this structure. We also discuss the possibility of this T#2 phase to exhibit stacking faults, whose amount depends on the method used to prepare this deintercalated phase.

Introduction

A metastable form of $LiCoO_2$ can be prepared by ion-exchange reaction. This phase was first prepared by Delmas et al. in 1982 from the P2-$Na_{0.70}CoO_2$ phase and was shown to exhibit an O2 stacking (AB CB oxygen packing) (Figure 1), with the cobalt ions in octahedral sites.[1] At that time, the structural study performed solely by X-ray diffraction (XRD) did not allow the localization of the lithium ions in the structure due to their low X-ray scattering factor, so the hexagonal *P*3*m*1 space group was used to describe the structure.

Two years later, Mendiboure et al. studied electrochemical deintercalation from O2-$LiCoO_2$ by XRD.[2] They reported that this system undergoes two reversible structural transformations during the deintercalation process: the first phase transition leads to the formation of another O2 phase, i.e., with the same stacking but different cell parameters (O2 ↔ O2* transformation), and the second phase transition observed for higher deintercalation amount leads to the formation of a new stacking called O6 (O2* ↔ O6 transformation). All these phases are named following the packing designation

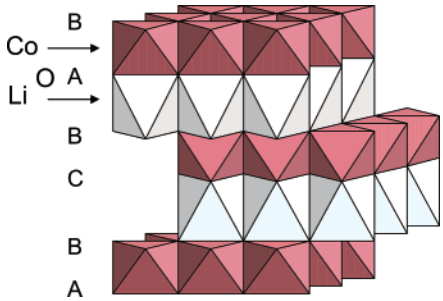

Figure 1. The O2 stacking of $LiCoO_2$.

proposed previously by Delmas et al. for the layered oxides: the P, T, or O letter describes the alkali ion site (prismatic, tetrahedral, or octahedral, respectively) and the number 1, 2, 3, ... indicates the number of slabs within the hexagonal cell.[3] Mendiboure et al. found the O2*-Li_xCoO_2 phase to be stable for $0.71 \leq x \leq 0.85$ and indexed its XRD pattern in the hexagonal system, using the *P*3*m*1 space group. Recently Dahn and colleagues also investigated the O2-$LiCoO_2$ system but used the more symmetrical $P6_3mc$ space group to describe the O2 stacking.[4] They performed in situ XRD to study the structural modifications observed for O2-$LiCoO_2$ upon lithium deintercalation and also observed the first reversible phase transition that leads to the formation of a phase which they called $O2_2$ ($O2_1$ ↔ $O2_2$ transforma-

* Corresponding author. Tel: +33-5-4000-2234. Fax: +33-5-4000-6698. E-mail: crog@icmcb.u-bordeaux.fr.
† Université Bordeaux I.
‡ Massachusetts Institute of Technology.

(1) Delmas, C.; Braconnier, J. J.; Hagenmuller, P. *Mat. Res. Bull.* **1982**, *17*, 117.
(2) Mendiboure, A.; Delmas, C.; Hagenmuller, P. *Mat. Res. Bull.* **1984**, *19*, 1383.
(3) Delmas, C.; Fouassier, C.; Hagenmuller, P. *Physica* **1980**, *99B*, 81.
(4) Paulsen, J. M.; Mueller-Neuhaus, J. R.; Dahn, J. R. *J. Electrochem. Soc.* **2000**, *147*, 508−516.

10.1021/ic026285t CCC: $27.50
Published on Web 01/03/2004

tion).[4] Two extra diffraction peaks indexed as (111) and (113) in the hexagonal system are observed for the $O2_2$ diffraction pattern: since they are forbidden in the $P6_3mc$ space group, it indicates that the structure of $O2_2$ differs from the starting O2 one. These authors, however, kept the $O2_2$ designation for this phase, as they did not study its structure precisely. At the same time, this group was studying the $Li_{2/3}Ni_{1/3}Mn_{2/3}O_2$ phase prepared by ion exchange,[5,6] which exhibits also the (111) and (113) XRD peaks. They fully characterized this phase, which exhibits a new stacking called T2. By analogy, in their study of the Li_xCoO_2 phases, they suggested that the appearance of these two peaks could be due to the gliding of every second CoO_2 slab by ($^1/_3$, $^1/_6$, 0),[4] which leads to the T2 structure.

Previously, we performed a detailed structural and physical characterization of the O2-$LiCoO_2$ system.[7,8] We showed by neutron diffraction, magnetic properties measurements, and ^{7}Li NMR that the starting O2-$LiCoO_2$ phase is stoichiometric with the lithium ions in the octahedral sites of the interslab space.[7] The strong electrostatic repulsion between Li^+ and Co^{3+} ions through the common face of their octahedra leads to a displacement of these ions from their ideal position.[7] Then, we studied the Li_xCoO_2 deintercalated phases from the viewpoint of structural and physical properties.[8] To better understand the unusual T#2 and O6 structures and the driving forces responsible for the phase tranformations observed upon lithium deintercalation, some of us have also performed a first principles study of the phase diagram of these layered Li_xCoO_2 phases deriving from O2-$LiCoO_2$.[9] They have shown for instance that the O2 → T#2 structural phase transformation is induced by enhanced configurational entropy in the T#2 phase and not by the metal−insulator transition. Moreover, two tetrahedral sites, 8e and $8f_{edges}$, need to be considered for the lithium ions in the T#2 domain in order to reach qualitative agreement with the experimental results.

As shown in Figure 2 by the cycling curve obtained for an Li//O2-$LiCoO_2$ cell, this T#2-Li_xCoO_2 phase, previously called O2* or $O2_2$ by other authors,[2,4] was found to be stable for $0.52 < x \leq 0.72$,[8] in good agreement with the results of Paulsen et al.[4] In our previous study, we showed using XRD, electronic properties, and ^{7}Li NMR that the O2 ↔ T#2 transformation is associated with a large increase in the interslab space and with a nonmetal to metal transition.[8] In the present paper, we focus on the structure of the T#2-Li_x-CoO_2 phase by using X-ray and neutron diffraction.

Experimental Section

Preparation of O2-$LiCoO_2$. The starting O2-$LiCoO_2$ phase was prepared by ion-exchange reaction from P2-$Na_{0.70}CoO_2$. The $Na_{0.70}$-CoO_2 precursor material was prepared by solid-state reaction from a mixture of Na_2O (Aldrich 99% min., 5% excess) and Co_3O_4 (obtained from $Co(NO_3)_2 \cdot 6H_2O$ Carlo Erba 99% minimum at 450°C for 12 h under O_2), which was ground and pelletized in a drybox (under argon), treated at 800°C under O_2 for 48 h, and then quenched into liquid N_2 in order to fix the oxygen stoichiometry. Ion-exchanging sodium for lithium in the P2 phase was performed in an aqueous solution of lithium salts.[7,11] An LiCl/LiOH (1:1) solution in water (5 M) was used and the exchange was carried out under refluxing conditions during 24 h with intermediate washing, drying, and grinding. A large excess of lithium was used (Li/Na = 10), and the exchanged phase was washed and dried under primary vacuum (10^{-2} Torr) at 100 °C for approximately 14 h.

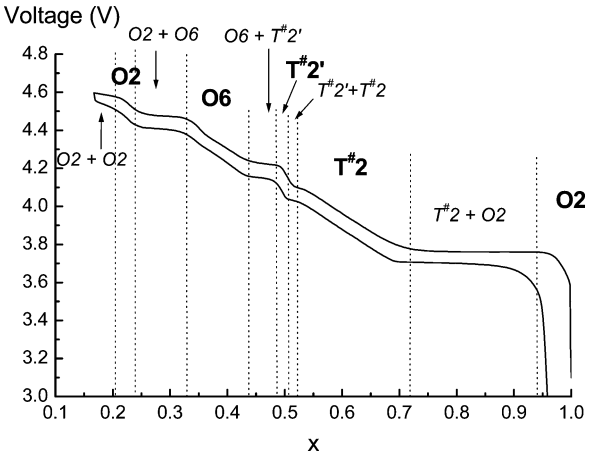

Figure 2. First galvanostatic charge−discharge curve of a Li//O2-$LiCoO_2$ cell obtained with a C/40 current density rate (40 h is needed to remove 1 mol of lithium).

Preparation of the T#2 Deintercalated Compounds. For the electrochemical preparation of the T#2 deintercalated compounds, Li/liquid electrolyte/O2-$LiCoO_2$ cells were used. $LiClO_4$ in propylene carbonate (1 M) was used as electrolyte. The cells were assembled in an argon-filled drybox.

As already described in ref 8, different kinds of mixtures were used as positive electrode, depending on the characterization carried out for the materials. For classical XRD experiments, a mixture of 86% by weight (wt %) active material, 4 wt % PTFE (polytetrafluorethylene), and 10 wt % graphite/carbon black (1:1) was used as positive electrode and the cells were charged at the C/40 rate (i.e. 40 h is needed to remove 1 mol of lithium). For XRD Rietveld acquisitions, a mixture of 90 wt % of active material and 10 wt % of graphite/carbon black (1:1) without binder was used as positive electrode. Large cells were used (≈700 mg of active material) and were charged at low current density (C/100). For ^{7}Li MAS NMR and electrical measurements, pellets (4 tons for an 8 mm diameter) of the starting material were used as positive electrode without additive and the cells were charged at very low current density (C/600). When charged to the wished compositions, all these positive electrodes were removed from the cells in an argon-filled drybox, washed with an excess of dimethyl carbonate, and then dried under vacuum.

For the neutron diffraction study, as a large amount of material is required, a T#2-Li_xCoO_2 compound was prepared by chemical deintercalation from the O2-$LiCoO_2$. A bromine solution in anhydrous acetonitrile (10 M) was used to extract lithium ions chemically. This solution is added in large excess (Br/Li = 10) to the O2-$LiCoO_2$ powder under an argon gas flow. The reaction was

(5) Paulsen, J. M.; Donaberger, R. A.; Dahn, J. R. *Chem. Mater.* **2000**, *12*, 2257−2267.
(6) Paulsen, J. M.; Dahn, J. R. *J. Electrochem. Soc.* **2000**, *147*, 2478−2485.
(7) Carlier, D.; Saadoune, I.; Croguennec, L.; Ménétrier, M.; Suard, E.; Delmas, C. *Solid State Ionics*, **2001**, *144*, 263−276.
(8) Carlier, D.; Saadoune, I.; Ménétrier, M.; Delmas, C. *J. Electrochem. Soc.* **2002**, *149* (10), A1310−A1320.
(9) Carlier, D.; Van der Ven, A.; Delmas, C.; Ceder, G. *Chem. Mater.* **2003**, *15*, 2651−2660.
(10) Lu, Dahn, J. R. *Chem. Mater.* **2001**, *13* (6), 2078−2083.
(11) Paulsen, J. M.; Thomas, C. L.; Dahn, J. R. *J. Electrochem. Soc.* **2000**, *147*, 2862−2867.

then carried out during 14 h with stirring. The deintercalated phase was finally washed with anhydrous acetonitrile, dried under vacuum, and kept in a drybox. The chemical analysis of this phase cannot be performed precisely as some P2-Na_xCoO_2 remains in the material. However, we estimate the lithium concentration to be close to $x = 0.56$ from the equilibrium potential (4.04 V) observed for the cell when this $T^{\#}2$-Li_xCoO_2 phase is used as starting active material.

X-ray Diffraction. The XRD patterns of the $T^{\#}2$ deintercalated phases were collected at room temperature from 10° to 120° (2θ) with a 0.02° step and a 40 s counting time by step, using a Siemens D5000 powder diffractometer with the Cu Kα radiation and a graphite diffracted beam monochromator. Simulations of the XRD patterns of materials with stacking faults were carried out using the DIFFaX program,[12] which calculates the diffracted intensity versus the 2θ value for a given stacking of slabs. As lithium is a poor XRD scatterer, it was not considered for the simulations. All the simulations considered a random distribution of stacking faults.

Neutron Diffraction. Neutron diffraction was performed at the Laue-Langevin Institute at Grenoble (France) on the high-resolution powder D2B diffractometer. The samples were contained in an 8 mm diameter vanadium tube. The diffraction pattern ($\lambda = 1.5940$ Å) was collected at room temperature from 0° to 162° (2θ) with a 0.05° step and a total counting time of 6 h. The crystal structure was refined by the Rietveld method using the Fullprof program.[13]

Due to the geometry of the neutron diffractometer (transmission mode), it was necessary to correct for the absorption in order to take into account a decrease of the experimental diffracted intensity compared to the expected one. To minimize this effect, the neutron diffraction pattern was collected on a ^{7}Li rich $T^{\#}2$-Li_xCoO_2 sample prepared by chemical deintercalation from enriched O2-$^7LiCoO_2$. The latter phase was prepared as described in ref 7. Indeed, the ^{6}Li isotope, which is 7.5% naturally abundant, absorbs 2×10^4 times more than the ^{7}Li one. The calculated absorption correction coefficient (μR factor in the Fullprof program) is equal to 0.44 for the studied $T^{\#}2$-$^7Li_xCoO_2$ phase. μ is the linear absorption coefficient of the sample and is defined as $\mu = (n/V)\sum_i n_i\sigma_i$, where n is the number of units in the unit cell, V the cell volume, n_i the number of a given atom in the unit, and σ_i the atomic absorption coefficient for the atom i. R is the radius of the cylinder defined by the sample studied.

Results and Discussion

XRD Study. Figure 3 shows the XRD patterns of the starting O2-$LiCoO_2$ phase and of the electrochemically deintercalated $T^{\#}2$-$Li_{0.61}CoO_2$ one (obtained from a positive electrode prepared with a mixture of 90 wt % active material and 10% graphite/carbon black (1:1), without binder). The indexation of the diffraction lines in the hexagonal system is also given in this figure. As noticed by Paulsen et al. and ourselves in previous papers, the patterns of O2 and $T^{\#}2$-Li_xCoO_2 look very similar, except at high diffraction angles with two extra diffraction lines for the latter.[4,8] These extra peaks are indexed in the hexagonal system as (111) and (113) and are situated around $2\theta = 67.5°$ and $2\theta = 73.4°$, respectively. As the appearance of these lines goes with the loss of the 6_3 symmetry axis, they are forbidden in the $P6_3mc$ space group and, therefore, the Li_xCoO_2 ($0.52 < x \leq 0.72$) compounds exhibit a structure different from the O2 one. By analogy with their study of the T2-$Li_{2/3}Ni_{1/3}Mn_{2/3}O_2$ phase,[5,6] Paulsen et al. suggested that the appearance of the (111) and (113) peaks could be due to the gliding of every second CoO_2 slab by ($^1/_3$, $^1/_6$, 0),[4] which leads to the $T^{\#}2$ structure. They, however, did not resolve the structure of the Li_xCoO_2 ($0.52 < x \leq 0.72$) phase. Besides their hypothesis, other glidings could also lead to the appearance of these two extra diffraction lines. To understand the first structural transformation occurring while deintercalating Li from O2-$LiCoO_2$, we performed several simulations of XRD patterns for structures deriving from the O2 one, using the DIFFaX program. Two CoO_2 hexagonal slabs (with $a = 2.8081$ Å and $c = 4.9512$ Å) were used: they are described in Table 1. These slabs were packed along the c-axis with a given translation vector, with an increasing gliding magnitude. The only stacking modifications that yield only to the appearance of the (111) and (113) peaks with the loss of the 6_3 symmetry axis are the gliding of every second CoO_2 slab.

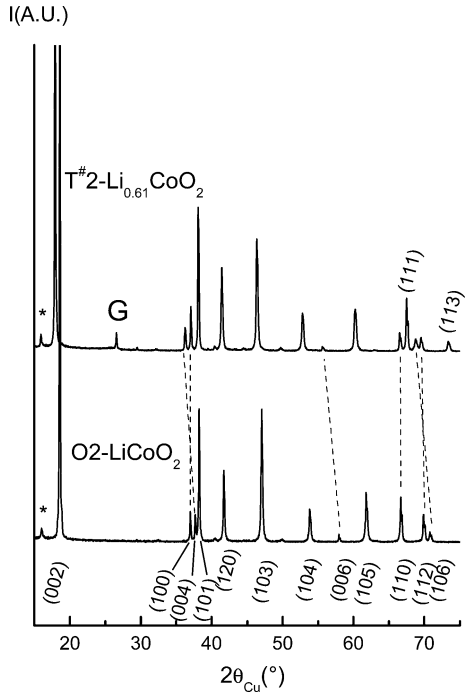

Figure 3. Comparison between the XRD patterns of the starting O2-$LiCoO_2$ phase and of the electrochemically deintercalated $T^{\#}2$-$Li_{0.61}CoO_2$ one. The asterisk symbol (*) indicates the position of the (002) peak of the remaining sodium phase. G = peak of graphite used as conducting agent in the positive electrode.

Table 1. Description of the Slabs Used To Simulate the XRD Patterns of the Structures Deriving from the O2 One by Gliding Every Second CoO_2 Slab in the ($^1/_2$, $^1/_2$, 0) or ($^1/_3$, $^1/_6$, 0) Directions[a]

hexagonal slabs $a = 2.8081$ Å, $c = 4.9512$ Å									
	slab 1					slab 2			
	x	y	z	occ		x	y	z	occ
Co	0	0	$^1/_2$	1	Co	$^2/_3$	$^1/_3$	$^1/_2$	1
O(1)	$^2/_3$	$^1/_3$	0.3	1	O (1)	0	0	0.3	1
O(2)	$^1/_3$	$^2/_3$	0.7	1	O (2)	$^1/_3$	$^2/_3$	0.7	1

[a] The simulations were made using the DIFFaX program, by packing the slabs along the c-axis with a given translation vector.

(12) Treacy, M. M. J.; Newsam, J. M.; Deem, M. W. *Proc. R. Soc. London Ser. A* **1991**, *43*, 499−520.
(13) Rodriguez-Carvajal, J. Laboratoire Léon Brillouin (CEA-CNRS), http://www-llb.cea.fr/fullweb/powder.html.

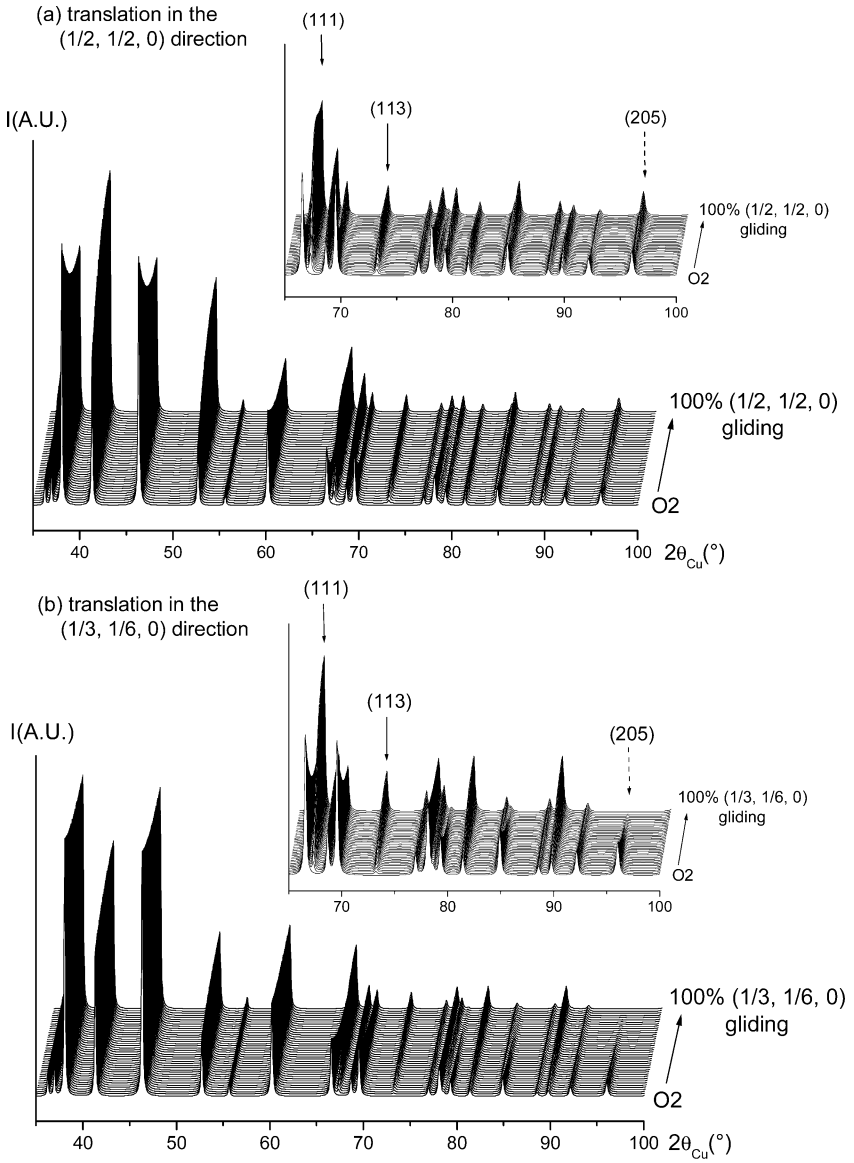

Figure 4. Simulated XRD patterns of structures deriving from O2 by gliding every second CoO_2 slab in the ($^1/_2$, $^1/_2$, 0) or ($^1/_3$, $^1/_6$, 0) directions, with an increasing gliding magnitude.

Figure 4 shows the XRD patterns calculated for the structures deriving from O2 by gliding of every second CoO_2 slab in the ($^1/_2$, $^1/_2$, 0) or ($^1/_3$, $^1/_6$, 0) directions, with increasing gliding magnitude. All these structures surprisingly exhibit quite similar XRD patterns, with the two extra diffraction lines as soon as the CoO_2 slab gliding occurs. Figure 5 shows the XRD patterns calculated for the two limit structures deriving from O2 by gliding every second CoO_2 slab by ($^1/_2$, $^1/_2$, 0) or ($^1/_3$, $^1/_6$, 0): they are the most similar to the experimental XRD pattern recorded for the T#2-Li$_{0.61}$CoO$_2$ phase. The obvious differences between the diagrams calculated for the structures resulting from the ($^1/_2$, $^1/_2$, 0) or ($^1/_3$, $^1/_6$, 0) gliding appear in relative peak intensities and also at high 2θ values with the (205) diffraction line observed at $2\theta = 96°$ for the former, whereas it is not for the latter. Comparison with the experimental pattern of T#2-Li$_{0.61}$CoO$_2$ shows that the structure resulting from the gliding of every second CoO_2 slab by ($^1/_3$, $^1/_6$, 0) is the most probable one for the T#2 structure. This result is in good agreement with the hypothesis made by Paulsen et al. for the O2$_2$-Li$_x$CoO$_2$ phase.[4] These simulations have clearly shown that completely different structures can lead to similar XRD patterns, emphasizing that one has to be careful for the structural characterization of phases from powder patterns, especially in these layered structures obtained upon lithium deintercalation by slab gliding and, therefore, usually characterized by stacking faults: indeed, only a small amount of stacking faults can strongly modify the relative peak intensities.[10]

Figure 6 shows the projection of the structure resulting from the ($^1/_3$, $^1/_6$, 0) gliding in the (110) plane. The two oxygen layers, above and below the lithium layer situated at $z = 0.25$, are displayed. It appears that, in the T#2 structure, the oxygen ions do not occupy the classical A, B, and C positions of a same triangular lattice anymore: as will be shown later in this paper, the lattice is orthorhombic and can be described in the *Cmca* space group. In this oxygen packing, the interslab space is built up of three types of tetrahedral sites which share faces (one 8e and two 8f)

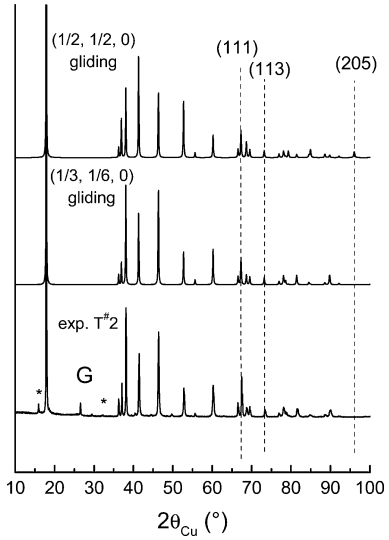

Figure 5. Simulated XRD patterns of the two limit structures deriving from O2 by gliding every second CoO_2 slab by ($^1/_2$, $^1/_2$, 0) or ($^1/_3$, $^1/_6$, 0), compared with the experimental XRD pattern recorded for the $T^{\#}2$-$Li_{0.61}CoO_2$ phase. The asterisk symbol (*) indicates the position of the major peaks of the remaining sodium phase. G = peak of graphite used as conducting agent in the positive electrode.

(Figures 6 and 7). Therefore, the lithium ions are in these tetrahedral sites that are unconventional in layered oxides. The very distorted 8e site shares an edge with one CoO_6 octahedron from one slab and another edge with one CoO_6 octahedron from the adjacent slab. The two 8f sites are somewhat less distorted: one shares three edges with CoO_6 octahedra from one slab and a corner with CoO_6 octahedra of the adjacent slab (it will be called $8f_{edges}$ in the following), whereas the other shares one face with one CoO_6 octahedron from one slab and a corner with three CoO_6 octahedra of the adjacent slab ($8f_{face}$). As in this structure the lithium ions occupy tetrahedral sites and as two layers are required to describe the unit cell, it was called $T^{\#}2$. The # symbol was used to discriminate this stacking from a T2 structure, in which the oxygen ions would occupy the positions of a same triangular lattice.

In our preliminary study performed by XRD,[8] the $T^{\#}2$ phase was described in the *Cmca* orthorhombic space group ($a = 2.80969(3)$ Å, $b = 4.84997(7)$ Å, $c = 9.9082(2)$ Å for $T^{\#}2$-$Li_{0.61}CoO_2$) with the cobalt and oxygen ions in 4a (0, 0, 0) and 8f (0, 0.162(2), 0.402(2)) positions, respectively. The lithium ions were fixed to the 8e sites ($^1/_4$, $^5/_{12}$, $^1/_4$) (the $8f_{edges}$ site position is approximatively (0, 0.833, 0.27)), by similarity with the assumption made by Paulsen et al. for the structure of the $Li_{2/3}Ni_{1/3}Mn_{2/3}O_2$ phase.[5, 6] Actually, the lithium position still needs to be confirmed. As adjacent 8e sites are very close, they cannot be occupied simultaneously. Due to the large number of available sites (2 positions for x lithium ions, with $0.52 \leq x < 0.72$), a lithium/vacancy ordering in the material should, therefore, be stabilized for peculiar compositions. A neutron diffraction study was carried out, to confirm the oxygen packing and to localize the lithium ions.

Neutron Diffraction Study. In our XRD study we have shown that the ($^1/_3$, $^1/_6$, 0) gliding allows one to describe nicely the experimental diffraction patterns. Nevertheless, to be sure that another packing could not be found, we decided to solve the structure ab initio from the neutron diffraction data.

A full pattern matching refinement (using the Fullprof program) was performed in order to fit a calculated profile to the experimental powder diffraction pattern (without the use of any structural model) by refinement of the lattice parameters, zero-point error, and pseudo-Voigt peak-shape parameters. A good minimization of the difference ($I_{obs} - I_{calc}$) was obtained with reliability factors R_{Bragg} and χ^2 equal to 2.66 and 2.77, respectively. Therefore, accurate values were determined from the fitted profile for the integrated peak intensities. These integrated intensities were then converted into structure factors (F) and used as input data for the sirpow program in order to solve the crystal structure by direct methods.[14] The standard input file for this program consists of lattice parameters ($a = 2.809$ Å, $b = 4.843$ Å and $c = 9.951$ Å), space group (*Cmca*), chemical content of the unit cell (at this step, only the dominant scatterers were considered, i.e. 4 Co and 8 O), and a file of reflections as provided by Fullprof [(hkl), multiplicity, sin θ/λ, 2θ, F^2]. Good results were obtained with the cobalt and oxygen atoms in the 4a (0, 0, 0) and 8f (0, ~0.160, ~0.400) positions, respectively.

The structural refinement by the Rietveld method was carried out by taking into account these results and, therefore, by assuming the following structural model: $(Co)_{4a}(O_2)_{8f}$ (space group *Cmca*). The y and z atomic positions of oxygen were refined, each site being fully occupied and the atomic displacement parameters (ADPs) of cobalt and oxygen being fixed to 0.5 Å^2 (typical value obtained for those kinds of elements in such structures). As expected (due to the missing lithium atoms in the structure), the minimization of the difference is obtained, but with rather high conventional Rietveld reliability factors R_{Bragg} and R_{wp} equal to 11.2% and 26.6%, respectively. From the Fourier difference maps ($z =$ 0.225, 0.25 and 0.275) presented in Figure 8, residual nuclear density was located in the 8e ($^1/_4$, ~0.42, $^1/_4$) position and attributed to lithium atoms in distorted LiO_4 tetrahedral sites.

At this step, we returned to the Rietveld refinement by taking into account the structural model $(Li_x)_{8e}(Co)_{4a}(O_2)_{8f}$. We refined the y and z atomic positions of oxygen, the y atomic position of lithium, the occupancy at the lithium site, and the ADPs of cobalt and oxygen, the cobalt and oxygen sites being fully occupied and the ADP of lithium being fixed to 0.5 Å^2 (typical value obtained for that kind of element in such structures). The corresponding calculated and experimental diffractograms are represented in Figure 9. Results of this refinement are given in Table 2. The introduction of lithium leads as expected to a very significative drop of the R values, $R_{Bragg} = 5.98\%$ and $R_{wp} = 12.1\%$, and to a good minimization of the difference ($I_{obs} - I_{calc}$). At this point, the Fourier difference maps show that no significant residual nuclear density remains. The oxygen packing proposed by Paulsen et al. for Li_xCoO_2 ($0.52 < x \leq 0.72$) and obtained

(14) Altomare, A.; Cascarano, G.; Giacovazzo, C.; Guagliardi, A. *J. Appl. Crystallogr.* **1994**, *27*, 435.

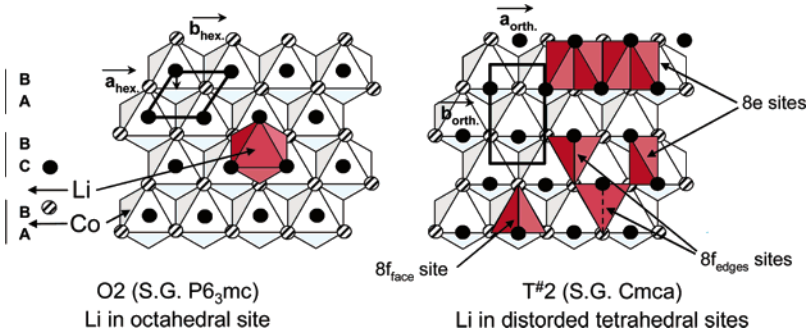

Figure 6. Projection in the (110) plane of the O2 and T#2 structures. The two oxygen layers, above (black) and below (hatched) the lithium layer situated at $z = 0.25$, are displayed. The lithium sites in O2 and T#2 structures are also shown.

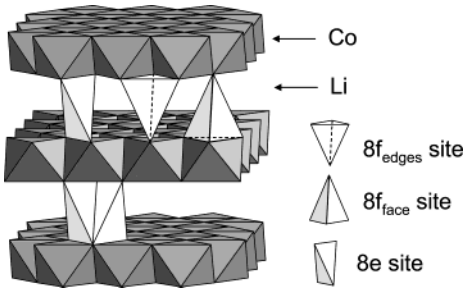

Figure 7. The T#2 stacking of Li$_x$CoO$_2$ phases ($0.51 < x \leq 0.72$). The distorted tetrahedral sites available for the lithium ions are also displayed.

Table 2. Structural Parameters Determined by the Rietveld Refinement of the T#2-Li$_{0.56}$CoO$_2$ Neutron and X-ray Diffraction Patterns[a]

T#2-Li$_x$CoO$_2$	
space group	*Cmca*
a	2.8088(3) Å/*2.8096(4) Å*
b	4.8430(5) Å/*4.8445(7) Å*
c	9.951(1) Å/*9.954(1) Å*

atoms	site	Wyckoff positions			B_{iso} (Å^2)	occupancy
Co	4a	0	0	0	0.0(1)	1
		0	*0*	*0*	*0.0(1)*	*1*
O	8f	0	0.1658(7)	0.4026(5)	0.28(6)	1
		0	*0.160(3)*	*0.400(1)*	*0.2(2)*	*1*
Li	8e	1/4	0.383(7)	1/4	0.5	0.28(3)
		1/4	*0.383*	*1/4*	*1.2*	*0.28*

Conditions of the Run

wavelength	1.5940 Å	step scan increment (2θ)	0.05°
temperature	300 K	zero point (2θ)	0.000(6)
angular range	$-7.45° \leq 2\theta \leq 162°$	no. of fitted parameters	19

Profile Parameters

Profile function	pseudo-Voigt $PV = \eta L + (1 - \eta)G$
$\eta = \eta_0 + X(2\theta)$	$\eta_0 = 0.70(6)/0.80(8)$
	$X = -/0.005(2)$
halfwidth parameters	$U = 0.24(4)/0.05(3)$
	$V = -0.16(6)/0.05(2)$
	$W = 0.11(2)/0.000(2)$

Conventional Rietveld *R*-Factors for Points with Bragg Contribution

$R_{wp} = 12.1\%/20.6\%$ $R_B = 5.98\%/4.42\%$

[a] The parameters obtained from the refinement of the XRD data are given in italics for comparison.

from O2 by the gliding of every second CoO_2 slab by ($1/3$, $1/6$, 0) is thus confirmed.[4]

The refinement shows that the occupancy at the lithium site is equal to 0.28 (i.e. Li$_{0.56}$CoO$_2$), in good agreement with previous assumptions based on the equilibrium potential (4.04 V) of the cell when this T#2-Li$_x$CoO$_2$ phase is used as starting active material.

Note that the residual nuclear density at the 8e position ($z = 0.25$) is distorted toward an 8f position underneath (see map with $z = 0.225$) and an 8f position above (see map with $z = 0.275$). These two 8f positions correspond to 8f$_{edges}$ tetrahedral sites that share one face with the 8e tetrahedral site, but no faces with CoO_6 octahedra. This result could suggest that, in this structure characterized by a large amount of available sites, there would be some mobility of the lithium ions with diffusion pathway 8e−8f$_{edges}$−8e−8f$_{edges}$−8e... as presented in Figure 8. Nevertheless, the refinement of the neutron data by the Rietveld refinement has shown that the presence of lithium in these 8f$_{edges}$ sites is not significant for this lithium concentration. This result is in agreement with previous first principles calculations that predicted a low occupation of the 8f$_{edges}$ site for concentration superior but close to $x = 0.5$, while an increase of the occupation was predicted for higher Li concentrations.[9]

This neutron diffraction study did not evidence extra reflections not taken into account by the cell proposed just before and, therefore, as expected, any Li/vacancy ordering in the interslab space. Indeed, $x = 0.56$ is not the best composition for characterizing a possible Li/vacancy ordering: $x = 0.50$, by similarity with the O3-LiCoO$_2$ system,[15] would have been probably a better choice, but this T#2-Li$_{0.50}$CoO$_2$ phase is difficult to prepare, especially in large amount as required for the neutron diffraction experiment. Moreover, note that simulations for T#2-Li$_{0.50}$CoO$_2$ of the theoretical neutron diffraction patterns for structures with Li/vacancy ordering in the interslab space have shown that the extra reflection intensities are too weak (comparable to the background noise) to be resolved by neutron diffraction.

The structural model obtained with the neutron data was used to refine the XRD data, the parameters concerning the lithium ions being fixed (i.e. Li$^+$ in 8e ($1/4$, 0.383, $1/4$) with a 0.28 occupancy). Indeed, due to the high accuracy of the wavelength, the cell parameters and atomic positions are better determined using XRD data. As shown in Table 2, the refinement of the XRD data by the Rietveld method confirmed the structural model $(Li_{0.56})_{8e}(Co)_{4a}(O_2)_{8f}$ for T#2-Li$_{0.56}$CoO$_2$, with similar structural parameters determined from neutron and X-ray diffraction data.

Stacking Faults. Figure 10 shows the XRD patterns obtained for several T#2-Li$_x$CoO$_2$ phases prepared under

(15) Reimers, J. N.; Dahn, J. R. *J. Electrochem. Soc.* **1992**, *139*, 2091−2097.

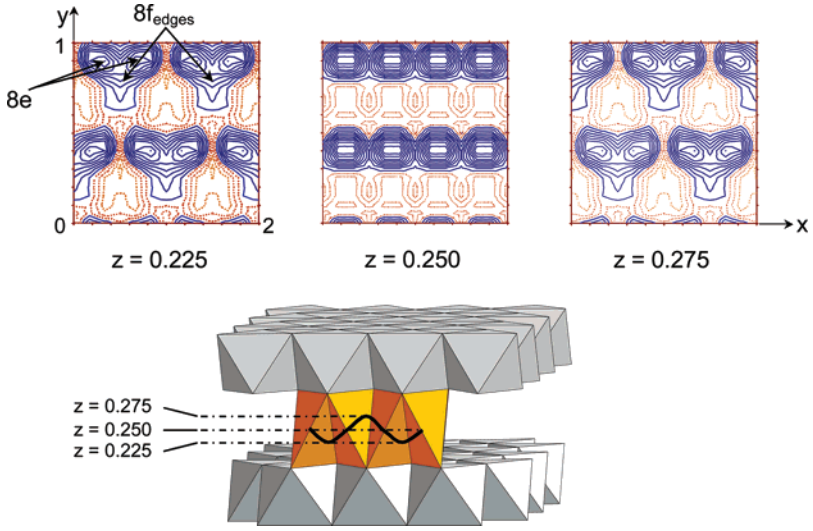

Figure 8. Fourier difference maps showing the residual nuclear density in planes parallel to the (001) plane, at $z = 0.225$, 0.25, and 0.275, when only Co and O are considered in the simulations. The remaining density corresponds to the Li nucleus.

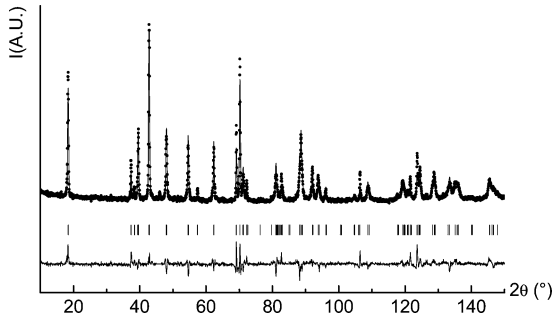

Figure 9. Comparison of the observed (●) and calculated (—) neutron diffraction patterns for T#2-$Li_{0.56}CoO_2$. The position of the (*hkl*) reflections and the difference curve are also given.

different conditions. All these phases exhibit a pattern characteristic of a T#2 structure, but with different peak widths, even if all these XRD patterns have been recorded with the same diffractometer (i.e. same instrumental broadening) and under the same conditions. The phase obtained by classical electrochemical deintercalation (Figure 10a), i.e., with graphite/carbon black and PTFE as additives, yields an XRD pattern which exhibits a strong preferential orientation: the (00*l*) peaks are clearly sharper and more intense than the other peaks. In the other three compounds, no PTFE was used and therefore it was possible to prepare the XRD samples in order to avoid any strong preferential orientation of the crystallites. The patterns of the phases obtained by electrochemical deintercalation from a pellet of $LiCoO_2$ without any additive (Figure 10b) or by chemical deintercalation (Figure 10c) both exhibit broader peaks than that observed for the phase obtained by electrochemical deintercalation with intermediate relaxation periods and the use of graphite/carbon black (Figure 10d). It appears thus that the peak width depends on the way used to prepare these phases.

Furthermore, the peak width of a given XRD pattern does not vary smoothly as a function of the scattering angle. Indeed, some peaks appear to be sharp (the (00*l*) and (131) peaks, for instance), whereas others are broader (the (11*l*) and (02*l*) peaks, for instance) (Figure 10). Most of the discrepancies observed between the experimental and the

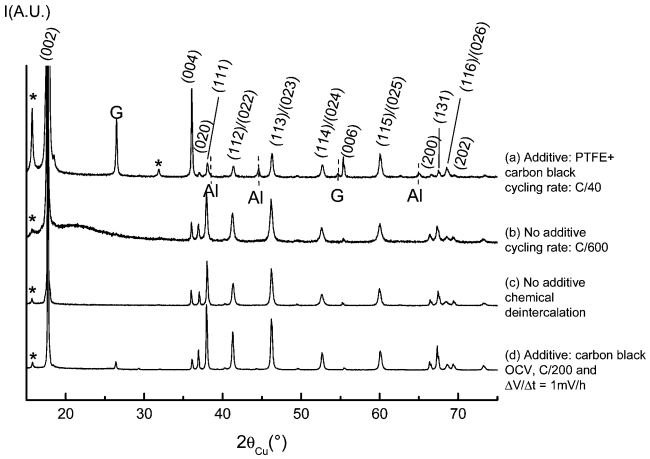

Figure 10. XRD patterns of several T#2 phases that differ from their way of preparation. (a) $Li_{0.55}CoO_2$ prepared by lithium electrochemical deintercalation (C/40) from a mixture of O2-$LiCoO_2$, graphite, carbon black, and PTFE. (b) $Li_{0.53}CoO_2$ prepared by lithium electrochemical deintercalation (C/600) from a pellet of pure O2-$LiCoO_2$. (c) $Li_{0.56}CoO_2$ prepared by chemical deintercalation of lithium. (d) $Li_{0.62}CoO_2$ prepared by lithium electrochemical deintercalation from a mixture of O2-$LiCoO_2$, graphite, and carbon black, with intermediate relaxation periods (C/200, 200 min charging, and $\Delta V/\Delta t = 0.1$ mV/h as criterion for the end of the relaxation period). Al indicates the position of the sample holder peaks, and the asterisk symbol (*) indicates a peak of carbon black. The peak indexation is done in the orthorhombic *Cmca* space group.

calculated neutron diffraction patterns displayed in Figure 9 are also due to this non-monotonous variation of fwhm versus 2θ.

Such non-monotonous peak width variation in diffraction patterns of layered compounds suggests the presence of stacking faults along the *c*-axis in these materials. To check this hypothesis, XRD patterns were simulated using the DIFFaX program. In Figure 11, we show the XRD patterns simulated in the presence of an increasing amount of O2 (a) or O6-type (b) stacking faults in the T#2 structure. These XRD patterns were calculated only with the Cu $K\alpha_1$ radiation. Orthorhombic slabs (with $a = 4.8450$ Å, $b = 2.8097$ Å, and $c = 4.9541$ Å) were used, four slabs (i.e. twice the "slab 1" and the "slab 2" given in Table 3) to describe the T#2 ↔ O2 phase transition and twelve slabs

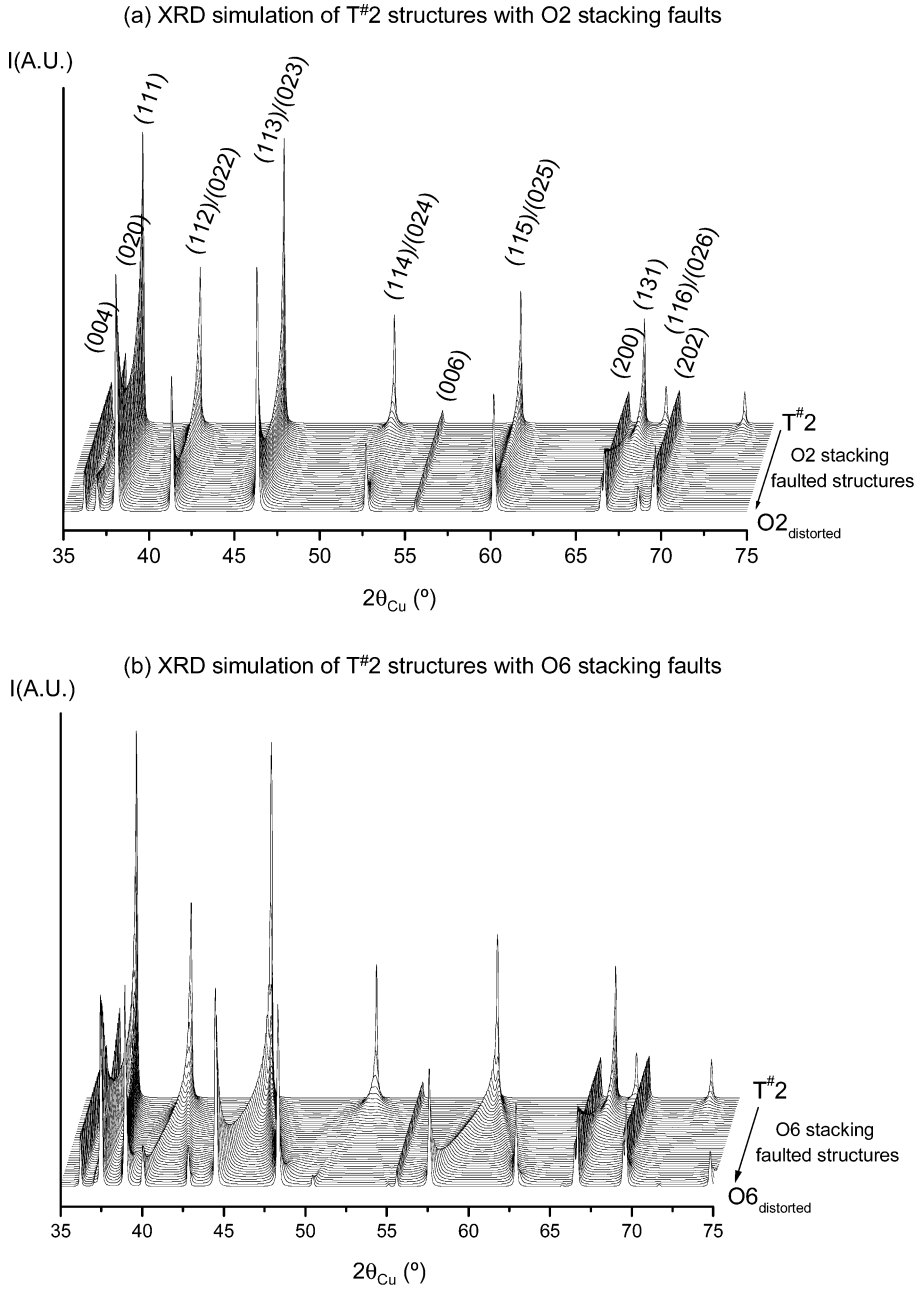

Figure 11. Evolution of the XRD pattern of a T#2 phase, with an increasing amount of O2 (a) and O6-type (b) stacking faults. The limit O2 and O6 structures are slightly distorted as orthorhombic slabs with T#2 cell parameters were used. The peak indexation is given in the *Cmca* space group.

(i.e. twice all the slabs given in Table 3) to describe the T#2 ↔ O6 phase transition. These slabs were packed along the *c*-axis with a given translation vector associated to a given probability. The number of stacking faults increases with a 2.5% step. In Figure 11, only the 35°−75° 2θ range is given; indeed the (002) peak is not affected by the presence of stacking faults, and no other peaks are located before $2\theta = 35°$. These simulations clearly show that, as experimentally observed for the T#2 XRD pattern, the (11*l*) and (02*l*) peaks are broadened if some O2 or O6-type stacking faults are present in the structure, whereas the (00*l*) are not affected. Note that the limit O2 and O6 structures are slightly distorted as orthorhombic slabs with T#2 cell parameters were used.

Figure 12 shows the experimental pattern of the phase prepared by OCV electrochemical deintercalation with a mixture of graphite and carbon black as additive, compared with those simulated for a T#2 structure without any stacking faults or with 2% of O2 or O6-type stacking faults. In that case, the two Cu $K\alpha_1$ and $K\alpha_2$ radiations were taken into account. It appears clearly that the experimental pattern is better simulated if a small amount of O2 or O6-type stacking faults is present in the T#2 structure. Note, however, that it is not possible to decide the nature of the stacking faults present in T#2. Indeed, the effects of a small amount of O2 or O6-type stacking faults on the XRD patterns are very similar. Nevertheless, note that the relative intensities of some peaks are still not well simulated [(114)/(024), (115)/(025) and (131), for example]. In a study to be published on the mechanism of the P2 → O2 transformation, we show that stacking faults can be formed at the junction of two domains

Table 3. Description of the Slabs Used To Simulate the XRD Patterns of T#2 Structures with O2 or O6-Type Stacking Faults[a]

orthorhombic slabs
$a = 4.8450$ Å, $b = 2.8097$ Å, $c = 4.9541$ Å

	slab 1					slab 2			
	x	*y*	*z*	occ		*x*	*y*	*z*	occ
Co(1)	0	0	1/2	1	Co (1)	1/3	0	1/2	1
Co(2)	1/2	1/2	1/2	1	Co (2)	5/6	1/2	1/2	1
O(1)	1/3	0	0.3	1	O(1)	0	0	0.3	1
O(2)	5/6	1/2	0.3	1	O(2)	1/2	1/2	0.3	1
O(3)	1/6	1/2	0.7	1	O(3)	1/6	1/2	0.7	1
O(4)	2/3	0	0.7	1	O(4)	2/3	0	0.7	1
	slab 3					slab 4			
	x	*y*	*z*	occ		*x*	*y*	*z*	occ
Co(1)	1/6	1/2	1/2	1	Co(1)	0	0	1/2	1
Co(2)	2/3	0	1/2	1	Co(2)	1/2	1/2	1/2	1
O(1)	0	0	0.3	1	O(1)	1/6	1/2	0.3	1
O(2)	1/2	1/2	0.3	1	O(2)	2/3	0	0.3	1
O(3)	1/3	0	0.7	1	O(3)	1/3	0	0.7	1
O(4)	5/6	1/2	0.7	1	O(4)	5/6	1/2	0.7	1
	slab 5					slab 6			
	x	*y*	*z*	occ		*x*	*y*	*z*	occ
Co(1)	1/3	0	1/2	1	Co (1)	1/6	1/2	1/2	1
Co(2)	5/6	1/2	1/2	1	Co (2)	2/3	0	1/2	1
O(1)	1/6	1/2	0.3	1	O(1)	1/3	0	0.3	1
O(2)	2/3	0	0.3	1	O(2)	5/6	1/2	0.3	1
O(3)	0	0	0.7	1	O(3)	0	0	0.7	1
O(4)	1/2	1/2	0.7	1	O(4)	1/2	1/2	0.7	1

[a] The simulations were made using the DIFFaX program, by packing the slabs along the *c*-axis with a given Translation vector and a given probability.

which have nucleated separately in the same crystal, the occurrence of the amount of stacking faults depending on the ratio between the nucleation and growth rates.[16] The same phenomenom could occur here since the nucleation and growth rates are a priori related to the electrode manufacturing and to the experimental conditions of the deintercalation. The T#2 phase thus appears to exhibit some stacking faults, whose amount depends on its preparation.

Conclusion

We undertook a detailed structural characterization of the T#2-Li_xCoO_2 ($0.52 < x \leq 0.72$) phases observed during the lithium electrochemical deintercalation form O2-$LiCoO_2$. We showed that this unusual stacking derives from the O2 one by gliding every second CoO_2 slab by ($1/3$, $1/6$, 0). By a neutron diffraction study, the lithium ions were evidenced to occupy very distorted tetrahedral sites in this structure, in good agreement with the predictions of the first principles calculations.

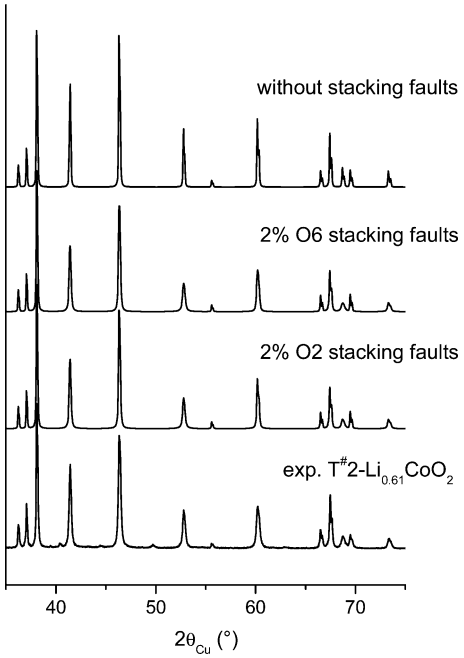

Figure 12. Comparison between the experimental pattern of the T#2-$Li_{0.61}$-CoO_2 phase, prepared by OCV electrochemical deintercalation with a mixture of graphite and carbon black as additive, and the patterns simulated for the T#2 structure without any stacking faults or with 2% of O2 or O6-type stacking faults.

The X-ray diffraction line profile was analyzed considering some stacking faults in the T#2 phase. It appears clearly that this phase exhibits a small amount of stacking faults whose amount depends on the method used to prepare this deintercalated phase.

Acknowledgment. The authors wish to thank Emmanuelle Suard and the Laue-Langevin Institute at Grenoble (France) for the neutron diffraction experiments, Ismaël Saadoune for fruitful discussions, and Cathy Denage for technical assistance. The Région Aquitaine, the French Ministry of Foreign Affairs (Lavoisier fellowship), and the NSF/CNRS exchange grants (INT-0003799) are thanked for financial support.

IC026285T

(16) Tournadre, F.; Croguennec, L.; Saadoune, I.; Carlier, D.; Shao-Horn, Y.; Willmann, P.; Delmas, C. Submitted to *J. Solid State Chem.*